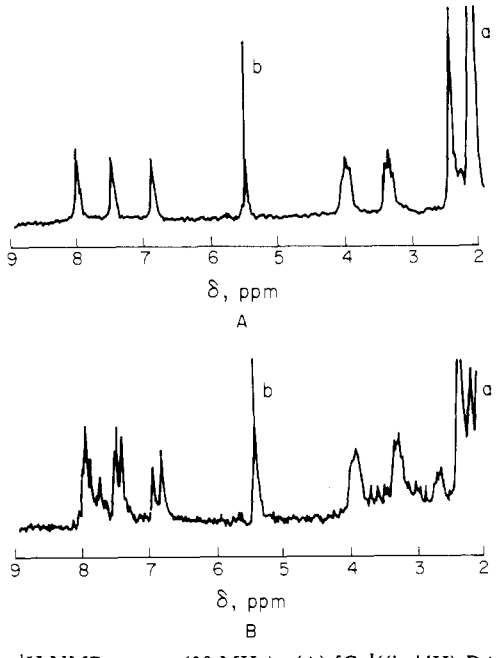

Figure 6. ^{1}H NMR spectra (90 MHz): (A) $[Cu^I((imidH)_2DAP)]^+$ in CD_3CN; (B) sample from part A after it was allowed to stand at room temperature under anaerobic conditions for 5 days. Extraneous peaks are labeled as follows: (a) supporting electrolyte, $(CH_3)_4NBF_4$;[5b] (b) contaminant CH_2Cl_2 from the drybox atmosphere.

ring that precludes ligand-arm cyclization of the nature found in $[Cu^I((imidH)(imidH)'DAP)]^+$.

With the realization that the oxygenation of $[Cu^I((imidH)_2DAP)]^+$ does not proceed reversibly as previously thought, the question remains as to the fate of $[Cu^I((imidH)_2DAP)]^+$ and O_2 upon reaction in their 2:1 stoichiometry. The postulated formation of an O_2 adduct as an intermediate ("Cu_2O_2") is still attractive.[4] However, the pathway by which regeneration of $[Cu^I((imidH)_2DAP)]^+$ (or something spectrophotometrically resembling this complex) occurs more likely results by disproportionation of "Cu_2O_2" to yield not only a Cu(I) complex but also $[Cu^{II}((imidH)_2DAP)]^{2+}$ and other unidentified product or products (brown material). The presence of a disproportionation reaction in the present case is supported by the fact that crystals of $[Cu^{II}((imidH)_2DAP)](BF_4)_2$ have been grown from oxygenated solutions of $[Cu^I((imidH)_2DAP)]^+$ (see Experimental Section) and verified to be the parent Cu(II) compound by X-ray diffraction methods. Shepherd and co-workers[34] have recently reported a detailed kinetic investigation of a binuclear vanadium complex with O_2 which also features a disproportionation mechanism that may have analogies to the present copper system. The brown material(s) obtained from oxygenation of the present $[Cu^I((imidH)_2DAP)]^+$ system has, to date, defied definitive identification, but efforts are continuing in this pursuit.[33]

Our earlier claim of reversibility in the oxygenation of $[Cu^I((imidH)_2DAP)]^+$ was based on a consistent set of data that, however, did not include the crucial test of an O_2-evolution experiment of the nature now described in this work. Conditions permitting, Toepler pump methodology offers one of the most direct and conclusive tests of O_2 reversibility, and it should continue to play a significant role in the development of new small molecule chemistry with Cu(I).

Acknowledgment. L.J.W. thanks the Robert A. Welch Foundation (Grant C-627) and the National Institutes of Health (Grant GM-28451) for support, D.M.S. thanks the NSF (Grant CHE-8520515) and the Robert A. Welch Foundation (Grant C-846) for support, and W.R.S. thanks the NIH (Grant GM-38401) for support. The Rigaku AFC-5 diffractometer at Rice was funded in part by an instrumentation grant from the National Science Foundation.

Registry No. $[Co^{II}(salen)]$, 14167-18-1; $[Cu^I((imidH)_2DAP)](BF_4)$, 75688-52-7; $[Cu^{II}((imidH)_2DAP)](BF_4)_2$, 82135-65-7; $[Cu^I((imidH)(imidH)'DAP)](BF_4)$, 117687-30-6; $(imidH)_2DAP$, 68940-73-8; (imidH)(imidH)'DAP, 117687-28-2; O_2, 7782-44-7.

Supplementary Material Available: Table SI, listing anisotropic temperature factors for $[Cu^I((imidH)(imidH)'DAP)]^+$ (1 page); listings of observed and calculated structure amplitudes for $[Cu^I((imidH)_2DAP)]^+$ and $[Cu^I((imidH)(imidH)'DAP)]^+$ (9 pages). Ordering information is given on any current masthead page.

(34) Myser, T. K.; Shepherd, R. E., *Inorg. Chem.* **1987**, *26*, 1544.

Contribution from the Departments of Chemistry, William Marsh Rice University, P.O. Box 1892, Houston, Texas 77251, Auburn University, Auburn, Alabama 36849, and University of Georgia, Athens, Georgia 30602

Ligand-Substitution and Electron-Transfer Reactions of Pentacoordinate Copper(I) Complexes

John A. Goodwin,[†] Lon J. Wilson,*[,†] David M. Stanbury,*[,‡] and Robert A. Scott[§]

Received May 3, 1988

The kinetics of the electron self-exchange for the Cu(I)/Cu(II) couple of the pentacoordinate complex of 2,6-bis[1-((2-imidazol-4-ylethyl)imino)ethyl]pyridine ($(imidH)_2DAP$) has been studied in CD_3CN by dynamic NMR line-broadening techniques. The rate constant, k'_{22}, is 1.31×10^4 M^{-1} s^{-1} at 25 °C and an ionic strength of 22.3 mM (Me_4NBF_4). Correction for ion pairing gives $k''_{22} = 2.8 \times 10^4$ M^{-1} s^{-1} at μ = 38 mM and 25 °C, which is a factor of 10 greater than that for the $[Cu((py)_2DAP)]^{n+}$ analogue. With the use of these two self-exchange rate constants, the Marcus cross relationship accurately predicts the measured cross-exchange rate constant. Transfer of the ligand from $[Cu^I((py)_2DAP)]^+$ to $[Zn^{II}(CH_3CN)_6]^{2+}$ at μ = 20 mM was investigated at 25 °C in CH_3CN by using the stopped-flow technique. With excess Zn(II), saturation kinetics were observed; this behavior is attributed to rate-limiting dissociation of the copper complex with a rate constant of 310 s^{-1}. These results are considered in evaluating the possibility of an inner-sphere mechanism of electron transfer.

Introduction

As the structural details of the Cu(I)/Cu(II) active sites of copper-containing proteins have become better known by X-ray crystallography,[1,2] understanding of the correlations of these structures with their outer-sphere electron-transfer rates has become a realistic goal. While the relatively high electron-self-exchange rate constants (10^4–10^6 M^{-1} s^{-1})[3-5] have been attributed

[†] William Marsh Rice University.
[‡] Auburn University.
[§] University of Georgia.

(1) (a) Guss, J. M.; Harrowell, P. R.; Murata, M.; Norris, V. A.; Freeman, H. C. *J. Mol. Biol.* **1986**, *192*, 361–387. (b) Guss, J. M.; Freeman, H. C. *J. Mol. Biol.* **1983**, *169*, 521–563.
(2) Norris, G. E.; Anderson, B. F.; Baker, E. N. *J. Am. Chem. Soc.* **1986**, *108*, 2784–2785.

0020-1669/89/1328-0042$01.50/0

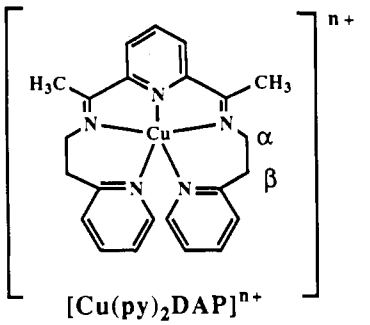

$[Cu(py)_2DAP]^{n+}$

A

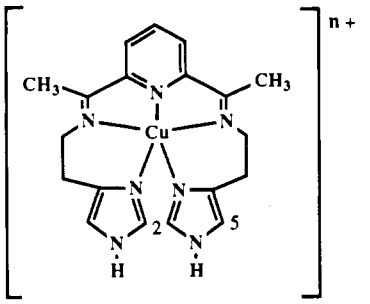

$[Cu(imidH)_2DAP]^{n+}$

B

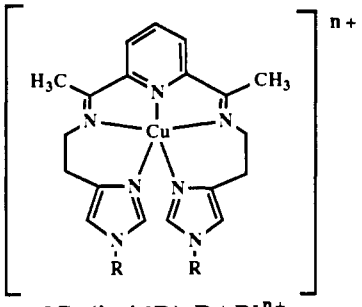

$[Cu(imidR)_2DAP]^{n+}$

C

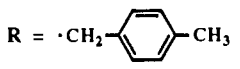

Figure 1. Schematic representations of the pentacoordinate copper complexes: (A) $[Cu((py)_2DAP)]^{n+}$; (B) $[Cu((imidH)_2DAP)]^{n+}$; (C) $[Cu((imidR)_2DAP)]^{n+}$.

to the small degree of active-site structural reorganization required in the outer-sphere redox processes,[6] separation of these effects from the contributions of other protein structural parameters has been limited due to the general complexity of the proteins. The "model compound" approach may be useful in generating concepts and deriving trends that can be applied to cuproproteins because of the relative ease in characterizing model compounds and the ability to control and simplify the factors governing reactivity.

Our recent structural and electron-transfer kinetic results for some pentacoordinate copper(I/II) model compounds[7] suggested that the $[Cu(L_2DAP)]^{n+}$ system,[8] depicted schematically in the compounds of Figure 1, shares an outer-sphere electron-transfer mechanism with the blue copper proteins by virtue of the retained coordination numbers in both +I and +II oxidation states. In that work, crystal structures were reported for the fluoroborate salts of $[Cu^{I/II}((py)_2DAP)]^{n+}$, and both oxidation states were found to be pentacoordinate. Measurement of the electron-self-exchange kinetics for this couple by dynamic NMR techniques yielded a value of 2.8×10^3 M^{-1} s^{-1} for k''_{11}, the self-exchange rate constant at 25 °C and ionic strength of 38 mM, corrected for ion-pairing. Electron-cross-exchange rates were measured for the reduction of $[Cu^{II}((py)_2DAP)]^{2+}$ by the analogous $[Cu^{I}((imidH)_2DAP)]^{+}$ and $[Cu^{I}((imidR)_2DAP)]^{+}$ complexes, and the Marcus theory was applied to estimate the self-exchange rate constants for the two couples as well. These calculated values were reported as $k''_{22} = 1.5 \times 10^4$ M^{-1} s^{-1} and $k''_{33} = 3.1 \times 10^4$ M^{-1} s^{-1}, respectively. The greater rate constants for these latter reactions were somewhat puzzling, but a detailed analysis was not possible because the structures of the Cu(I) complexes were unknown.

Subsequently, a determination of the crystal structure of $[Cu^{I}((imidH)_2DAP)]^{+}$ has demonstrated that this member of the $[Cu(L_2DAP)]^{n+}$ series is also pentacoordinate in both oxidation states.[9,10] Presented here are direct measurements of the self-exchange electron-transfer rate for this $[Cu^{I,II}((imidH)_2DAP)]^{n+}$ couple by dynamic NMR techniques. These results now afford an opportunity to examine the structure/reactivity question for these pentacoordinate copper species in greater detail. Also reported herein are ligand-substitution kinetic results that probe the possibility of an inner-sphere mechanism in the electron-transfer process. Finally, EXAFS studies are also presented in order to clarify the nature of the species in the solution state.

Experimental Section

Materials. Acetonitrile (Burdick & Jackson) was predried over 4-Å molecular sieves before distillation from $CuSO_4$ and a second distillation from CaH_2. Both distillations were carried out under N_2, and only the middle 80% fractions were collected. Dioxygen removal was achieved by using argon sparge before storage under N_2. Acetonitrile-d_3 (Aldrich, 99% isotopic purity) used in the $1/T_2$ NMR measurements was degassed by the freeze–pump–thaw technique at 0.01 mTorr on a high-vacuum line. Propylene carbonate (PC) (Aldrich) was twice distilled at 1 Torr and 110 °C; $CaSO_4$ was added to the flask for the first distillation only. A lower boiling fraction, which was obtained in the first distillation only, was discarded. After being degassed with argon sparge, the solvent was stored under N_2 in a N_2-filled drybox (Vacuum Atmospheres Co.).

The copper(II) complexes of 2,6-bis[1-((2-imidazol-4-ylethyl)imino)ethyl]pyridine ($(imidH)_2DAP$)[8] and 2,6-bis[1-((2-pyridin-2-ylethyl)imino)ethyl]pyridine ($(py)_2DAP$)[8] and Me_4NBF_4 were prepared and recrystallized as described previously.[7]

$[Cu^{I}(imidH)_2DAP)](BF_4)$ and $[Cu^{I}((py)_2DAP)](BF_4)$ stock solutions for the kinetics studies were prepared anaerobically as described previously[7] by electrosynthetically reducing their Cu(II) analogues in PC or CH_3CN with 50 mM n-Bu_4NBF_4 as the supporting electrolyte.

Electrochemically prepared $[Cu^{I}((imidH)_2DAP)](BF_4)$ was isolated as follows. The reduction was performed in CH_3CN with $NaBF_4$ as the supporting electrolyte. After removal of the solvent, the mixed solids were transferred in a Schlenk flask under vacuum to the drybox. The material was then purified by using a minimum amount of CH_3CN to dissolve all solids, followed by addition of CH_2Cl_2 to precipitate the $NaBF_4$ from the deep red solution. The resulting suspension was then filtered, and cyclohexane was added to the solution to yield a fine red-brown precipitate. The red powder was collected by filtration and then evacuated at room temperature for 6–8 h to remove any remaining solvent prior to its use in the NMR experiments.

(3) Groeneveld, C. M.; Dahlin, S.; Reinhammar, B.; Canters, G. W. *J. Am. Chem. Soc.* **1987**, *109*, 3247–3250.
(4) Armstrong, F. A.; Driscoll, P. C.; Hill, H. A. O. *FEBS Lett.* **1985**, *190*, 242–248.
(5) Dahlin, S.; Reinhammar, B.; Wilson, M. T. *Biochem. J.* **1984**, *218*, 609–614.
(6) Gray, H. B.; Malmstrom, B. G. *Comments Inorg. Chem.* **1983**, *2*, 203–209.
(7) Goodwin, J. A.; Stanbury, D. M.; Wilson, L. J.; Eigenbrot, C. W.; Scheidt, W. R. *J. Am. Chem. Soc.* **1987**, *109*, 2979–2991.
(8) The abbreviation nomenclature does not follow IUPAC conventions in that the (py), (imidH), and (imidR) designations do not refer to pyridine, imidazole, and N-substituted imidazole as intact species. In all cases, diacetylpyridine (DAP) has undergone Schiff base condensation, and it is not a discrete ligand. The compounds $[Cu((imidH)_2DAP)]^{2+/+}$ and $[Cu((py)_2DAP)]^{2+/+}$ have previously had the designations $[Cu(imep)]^{2+/+}$ and $[Cu(pyep)]^{2+/+}$.
(9) Goodwin, J. A.; Bodager, G. A.; Wilson, L. J.; Stanbury, D. M.; Scheidt, W. R. *Inorg. Chem.*, preceding paper in this issue.
(10) Korp, J. D.; Bernal, I.; Merrill, C. L.; Wilson, L. J. *J. Chem. Soc., Dalton Trans.* **1981**, 1951–1956.

n-Bu_4NBF_4 (Aldrich) was recrystallized from ethyl acetate with hexane. The white crystals were washed with diethyl ether and dried at 80 °C under vacuum.

$[Zn^{II}(CH_3CN)_6](BF_4)_2$ was prepared by a modification of the procedure of Hathaway et al.[11] in which a suspension of excess powdered zinc metal (Baker) in dry CH_3CN reacted with dissolved $NOBF_4$ (Aldrich) on a Schlenk line under vacuum. The reaction proceeded with evolution of NO gas, which was trapped at liquid N_2 temperatures as a blue liquid. Upon the cessation of gas evolution, the solution was transferred to the drybox, filtered to remove the zinc metal, and then lyophilized to yield a low-melting white solid, which had high solubility in CH_3CN and which was very hygroscopic. Crystalline $[Zn^{II}(CH_3CN)_6](BF_4)_2$, used in the kinetic studies, was prepared by recrystallizing the crude product in the drybox from very concentrated, deep yellow, viscous solutions in hot CH_3CN. The crystals were collected by cooling the hot solution in a funnel with a fine-fritted glass disk. Removal of the viscous mother liquor was carried out by extended ($\approx^1/_2$ h) filtration. The resulting product retained the low melting point (57 °C) and high solubility in CH_3CN. If the crystalline product was washed with ethyl acetate as recommended[11] or vacuum-dried at room temperature, both of these characteristic properties were lost due to decomposition by solvent loss. Therefore, both of these procedures were avoided. The crystals, slightly moist with excess solvent, were used in the ligand-exchange experiments, so solutions prepared from them required standardization (vide infra).

$[Zn^{II}(H_2O)_6](BF_4)_2$ (Alfa) was used without purification, and $[Zn^{II}((py)_2DAP)](BF_4)_2$ was prepared as described previously.[12]

Electrochemical reduction was carried out by using a BAS SP-2 potentiostat with a PAR Model 379 digital coulometer and an Industrial Scientific Omniscribe strip-chart recorder. A platinum-mesh working electrode, a Ag/AgCl reference electrode, and a small platinum-mesh counter electrode were used in a cell assembly constructed for anaerobic handling of solutions.

X-ray Absorption Measurements. X-ray absorption spectroscopic data were collected at the Stanford Synchrotron Radiation Laboratory under dedicated operating conditions (3.0 GeV, ≈60 mA) on wiggler beam line VII-3 by using standard transmission techniques, including internal energy calibration.[13]

Variable-Temperature NMR Measurements. Temperature-dependent ^1H NMR spectra of $[Cu^I((py)_2DAP)]^+$ in CD_2Cl_2 were taken with an IBM 300-MHz spectrometer over the temperature range 273–193 K at 20 K intervals. The 10 mM sample was contained in a 5-mm tube fitted with a Teflon stopcock cap (Wilmad).

Determination of Ligand-Substitution Products. The products of the reactions of $[Cu^I((py)_2DAP)]^+$ with Zn^{2+} were examined by ^1H NMR spectroscopy. The products were prepared by in situ anaerobic reactions of the Cu(I) complex with $[Zn^{II}(H_2O)_6](CF_3SO_3)_2$ (Alfa) in CD_3CN and also similarly with $[Zn^{II}(CH_3CN)_6](BF_4)_2$ to avoid possible problems associated with excessive water contamination. These spectra were compared to that of $[Zn^{II}((py)_2DAP)](BF_4)_2$ in CD_3CN, which had been characterized previously.[12]

Ligand-Substitution Kinetics. Standardizations of the Zn^{2+} stock solutions used in the kinetics studies were performed by using a colorimetric method with aqueous Zincon[14] (Aldrich) at pH = 9.0 in a borate–HCl buffer with $[Zn^{2+}] \approx 0.02$ mM by dilution of the CH_3CN solution with water. The kinetics of the reactions of the Cu(I) complexes $[Cu^I((imidH)_2DAP)]^+$ and $[Cu^I((py)_2DAP)]^+$ with excess Zn^{2+} was measured by the stopped-flow method, monitoring the loss of absorbance of the copper complexes at the appropriate λ_{max} (480 nm for the $((py)_2DAP)$ complex and 510 nm for the $((imidH)_2DAP)$ complex). A Hi-Tech Scientific Model SF-51 stopped-flow apparatus (with a SU-40 spectrophotometric unit and a Model C-400 circulating temperature bath) was used in conjunction with the OLIS 3820 data acquisition system described earlier.[7]

Anaerobic conditions were maintained in the kinetics solutions by using standard syringe techniques as previously described.[7] The stopped-flow apparatus was fitted with glass luer-tipped transfer tubes, which allowed the filling syringes to be joined directly to the driving syringes. Nylon three-way stopcocks were used to seal these transfer tubes between fillings and were rinsed with fresh argon-saturated solutions before injection into the driving syringes. The circulating water of the temperature bath that surrounded the flow circuit was sparged with argon to minimize air contamination.

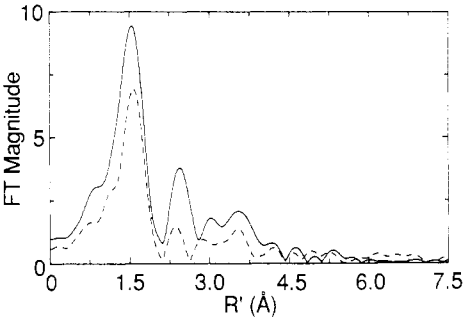

Figure 2. Fourier transforms (k = 3.0–13.0 Å^{-1}, k^3 weighting) of Cu EXAFS data for $[Cu^I((imidH)_2DAP)]^+$ (- - -) and $[Cu^{II}((imidH)_2DAP)]^{2+}$ (—) in CH_3CN at −30 °C.

The dependence of the observed rate upon the concentration of the excess Zn^{2+}, as both the CH_3CN solvate and also as the hydrated complex, was examined over the range of Zn^{2+} concentrations from 0.25 to 2.5 mM. With the CH_3CN complex, two separate levels of constant ionic strength, 10 and 20 mM, were investigated by using n-Bu_4NBF_4 as the background electrolyte. The reported ionic strengths include corrections for ion pairing of the background electrolyte,[15] K_{IP} = 10 M^{-1}, as well as ion pairing of the zinc CH_3CN solvate, with K_{IPZn} = 126 M^{-1}.[16] The reaction with $[Cu^I((py)_2DAP)]^+$ gave well-behaved pseudo-first-order kinetic decays, and rate constants were determined from the negative slopes of the plots of log $(A_t - A_\infty)$ vs time by using the data manipulation routines available on the OLIS system.

Electron-Self-Exchange Rate Measurements. The samples of $[Cu^I((imidH)_2DAP)](BF_4)$ (7.3 mM) in CD_3CN with varying concentrations of $[Cu^{II}((imidH)_2DAP)](BF_4)_2$ and Me_4NBF_4 for μ = 22.3 mM, were prepared in the drybox by using the solid Cu(I) salt. The samples were prepared in 5-mm NMR tubes (Wilmad, precision grade) with 9-mm O-ring-jointed vacuum-line connections and Teflon needle valves. After the valves were closed, the tubes were removed from the drybox, subjected to freeze–pump–thaw degassing on a vacuum line and then sealed below the valve with a torch. The sealed samples were kept frozen in liquid N_2 until just before the NMR experiments were conducted.

Determinations of $1/T_2$ for each sample were made by measuring the line width of the homonuclear spin-decoupled ^1H resonance of the 5-position proton (Figure 1B) of the imidazole moiety at δ = 6.9. The spectra were obtained by using a JEOL FX-90Q spectrometer operating at 89.6 MHz with a frequency bandwidth of 1800 Hz described by 16K data points. An exponential window function, which was applied to the 500 time domain accumulations, introduced line broadening of 0.4898 Hz; this contribution was taken into account in determining the line width. Zero-point filling of the last 5600 points of the FID was also used to minimize noise. Homonuclear proton decoupling was achieved by irradiating the N-bound imidazole proton resonance, which appeared in a variable position around 10–11 ppm. The sample temperature was maintained at 25 °C with the JEOL temperature control unit.

Numerical Methods. Kinetics data analyses were carried out by using the Los Alamos nonlinear least-squares program. Linear fits of the dependence of $1/T_2$ upon [Cu(II)] used weighting inverse to the dependent variable.

Results

Solution-State Structures. As reported elsewhere,[9] the crystal structure of $[Cu^I(imidH)_2DAP)]^+$ has a pentacoordinate geometry similar to that of the Cu(II) analogue.[10] The structures of these complexes in solution are not necessarily the same as those in the solid state. Both EXAFS and NMR spectroscopy are used to address this issue below.

(A) EXAFS Results. In a previous report[17] EXAFS data on $[Cu((imidH)_2DAP)]^{n+}$ were presented and analyzed in terms of the reactivity of Cu(I) with O_2. With a crystal structure now available for the Cu(I) form of the compound,[9] it is of interest to reexamine the EXAFS data in terms of the solution-state

(11) Hathaway, B. J.; Holah, D. G.; Underhill, A. E. *J. Chem. Soc.* **1962**, 2444–2448.
(12) Merrill, C. L.; Wilson, L. J.; Thamann, T. J.; Loehr, T. M.; Ferris, N. S.; Woodruff, W. H. *J. Chem. Soc., Dalton Trans.* **1984**, 2207–2221.
(13) Scott, R. A. *Methods Enzymol.* **1985**, *117*, 414–459.
(14) (a) Snell, F. D. *Photometric and Fluorometric Methods of Analysis: Metals, Part 2*; Wiley: New York, 1978; p 1063. (b) Rush, R. M.; Yoe, J. H. *Anal. Chem.* **1954**, *26*, 1345–1347.
(15) Nielson, R. M.; Wherland, S. *Inorg. Chem.* **1984**, *23*, 1338–1344.
(16) Libus, W.; Chachulski, B.; Fraczyk, L. *J. Solution Chem.* **1980**, *9*, 355–369.
(17) Goodwin, J. A.; Stanbury, D. M.; Wilson, L. J.; Scott, R. A. In *Biological & Inorganic Copper Chemistry*; Karlin, K. D., Zubieta, J., Eds.; Adenine Press: Guilderland, NY, 1986; Vol. 2, pp 11–25.

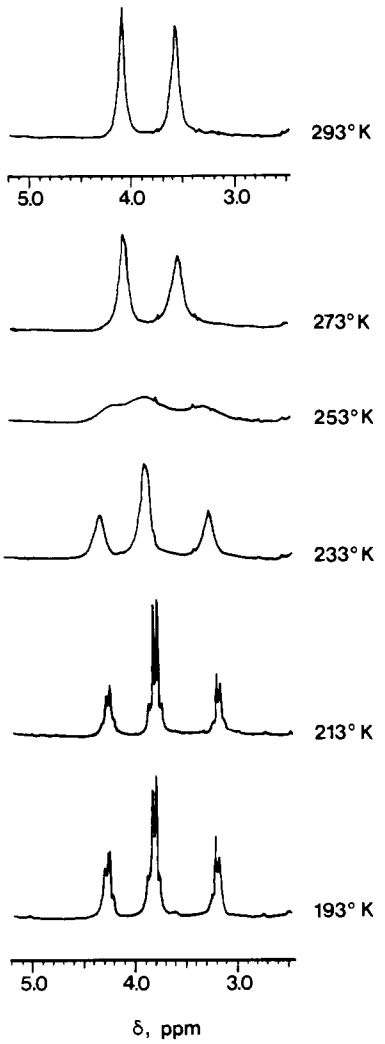

Figure 3. Variable-temperature ^1H NMR spectra (300 MHz) in the proton methylene region for $[Cu^I((py)_2DAP)]^+$ in CD_2Cl_2.

coordination numbers. Figure 2 shows the Fourier transforms (FTs) of the Cu(I) and Cu(II) complexes in CH_3CN. The Cu(I) compound shows significantly reduced intensity, both in the main (first-shell) and the outer-shell FT peaks, with the reduction in intensity being much more severe in the second FT peak. Curve fitting the first-shell filter for the Cu(II) compound showed that only one Cu–(N,O) shell was needed with a coordination number of 5 at a distance of 2.00 Å (the crystallographic average is 2.02 Å). A similar fit of the Cu(I) compound was particularly poor. A much better fit of the first-shell filter was obtained by assuming that the Cu(I) coordination sphere could be thought of as two separate shells (three N at 1.91 Å and two N at 2.40 Å)[9] and that the three shorter Cu(I)–N interactions made up the main FT peak. The much reduced intensity of the second FT peak can be interpreted as due to destructive interference between the two longer Cu(I)–N bonds and the second-shell Cu(I)···C interactions. Thus the EXAFS data are consistent with a model in which the solution- and solid-state structures are similar. No EXAFS data are currently available for the $[Cu((py)_2DAP)]^{n+}$ complexes.

(B) NMR Results. The room-temperature ^1H NMR spectrum of the methylene proton region for $[Cu^I((py)_2DAP)]^+$ in CD_2Cl_2, displayed in Figure 3, is similar to that previously reported in CD_3CN,[7] except that the weak couplings of the α and β methylene protons at 4.13 and 3.56 ppm are not resolved. Because the molecule is chiral and because the X-ray crystal structure shows that the two arms of the ligand are not equivalent, in principle a total of eight inequivalent methylene protons exist in the molecule. Since only two resonances are seen, apparently at room temperature the two arms of the ligand are equivalent, unlike in the crystal structure; moreover, the two protons of each methylene group are also equivalent, which indicates that the molecule must be undergoing a rapid racemization. The two peaks broaden as the temperature is lowered to −20 °C, and when the temperature is lowered further to −80 °C, they split and sharpen to yield three unevenly spaced multiplets of intensity 1:2:1; the other portions of the NMR spectrum are essentially temperature independent. This behavior in the methylene proton region is interpreted as arising from two doublets of multiplets in which two of the multiplets overlap accidentally. Coaslescence occurs at ca. −20 (±10) °C for both doublets, and the peak separations of the finally-resolved methylene resonances are approximately 110 and 180 Hz. These peak separations are related to the lifetimes, τ', at the coalescence temperatures according to[18]

$$\tau' = 2^{1/2}/2\pi(\nu_a^\circ - \nu_b^\circ) \quad (1)$$

which leads to lifetimes of 2.1 and 1.3 ms. Presumably these lifetimes pertain to the same rate process and reflect slightly different coalescence temperatures. We take these results to indicate that the process has a rate constant of about 400 s^{-1} near 253 K in CD_2Cl_2. The approximate equivalence of the relative populations of the coalescing methylene protons strongly suggests that the process leading to the temperature dependence is a racemization of the complex. Even at the lowest temperatures attained, we see no evidence for a slowing of the presumed motion that makes both arms of the ligand equivalent. The racemization mechanism probably involves a partial ligand dissociation and reassociation, proceeding by way of a four-coordinate intermediate at undetectably low concentration.

Reactions with Entering Ligands. Preliminary studies of some substitution reactions of Cu(I) with entering ligands have been performed and are described in detail elsewhere.[19] The reactions studied were those of $[Cu^I((py)_2DAP)]^+$ and $[Cu^I((imidH)_2DAP)]^+$ with 2,9-dimethylphenanthroline and 4,7-dimethylphenanthroline in acetonitrile and in propylene carbonate. In all cases the reactions with excess phenanthroline led to rapid and complete displacement of the pentadentate ligand by the phenanthroline. When the reactions were investigated by stopped-flow UV–vis spectrophotometry they were found to proceed with pseudo-first-order kinetics, but the absorbance change during this process was only a fraction of that expected: i.e., a substantial portion of the overall absorbance change occurred in a prior step that was too rapid to monitor. The dependence of the detectable step on the concentration of the entering ligand was found to be complicated and variable, depending on the solvent, ligand, and complex. It was assumed that these reactions were proceeding by a rapid association of the phenanthroline with the complex, followed by a slower associative displacement of the ligand, but further studies were not undertaken.

Metal-Exchange Reactions. Several substitution reactions of the Cu(I) complexes with solvated metal ions were investigated in acetonitrile as discussed below.

(A) Product Determinations. The reaction of $[Cu^I((py)_2DAP)]^+$ with $[Zn^{II}(CH_3CN)_6]^{2+}$ gave a product NMR spectrum consistent with ligand transfer from Cu(I) to Zn(II), as shown in Figure 4A,B. However, when $[Zn(H_2O)_6]^{2+}$ was used as the source of Zn(II), the product NMR spectrum was not as simple as for the $[Zn(CH_3CN)_6]^{2+}$ case, possibly because of hydrolysis of the imine linkage in the ligand. This spectrum is shown in Figure 4C. The apparent course of this reaction was unexpected and was further probed by obtaining the spectrum of $[Zn^{II}((py)_2DAP)]^{2+}$ in the presence of $[Zn^{II}(H_2O)_6]^{2+}$ and $[Cu^I(CH_3CN)_4]^+$. These additions had no effect upon the spectrum of $[Zn^{II}((py)_2DAP)]^{2+}$, suggesting that the hydrolysis reaction occurs during the ligand exchange. The kinetics studies, described below, utilized $[Zn^{II}(CH_3CN)_6]^{2+}$ to avoid this complication. The overall absorbance

(18) (a) Drago, R. S. *Physical Methods in Chemistry*; W. B. Saunders: Philadelphia, PA, 1977; pp 252–259 and references therein. (b) Groeneveld, C. M.; van Rijn, J.; Reedijk, J.; Canters, G. W. *J. Am. Chem. Soc.* **1988**, *110*, 4893–4900.
(19) Goodwin, J. A. Ph.D. Dissertation, William Marsh Rice University, 1987.

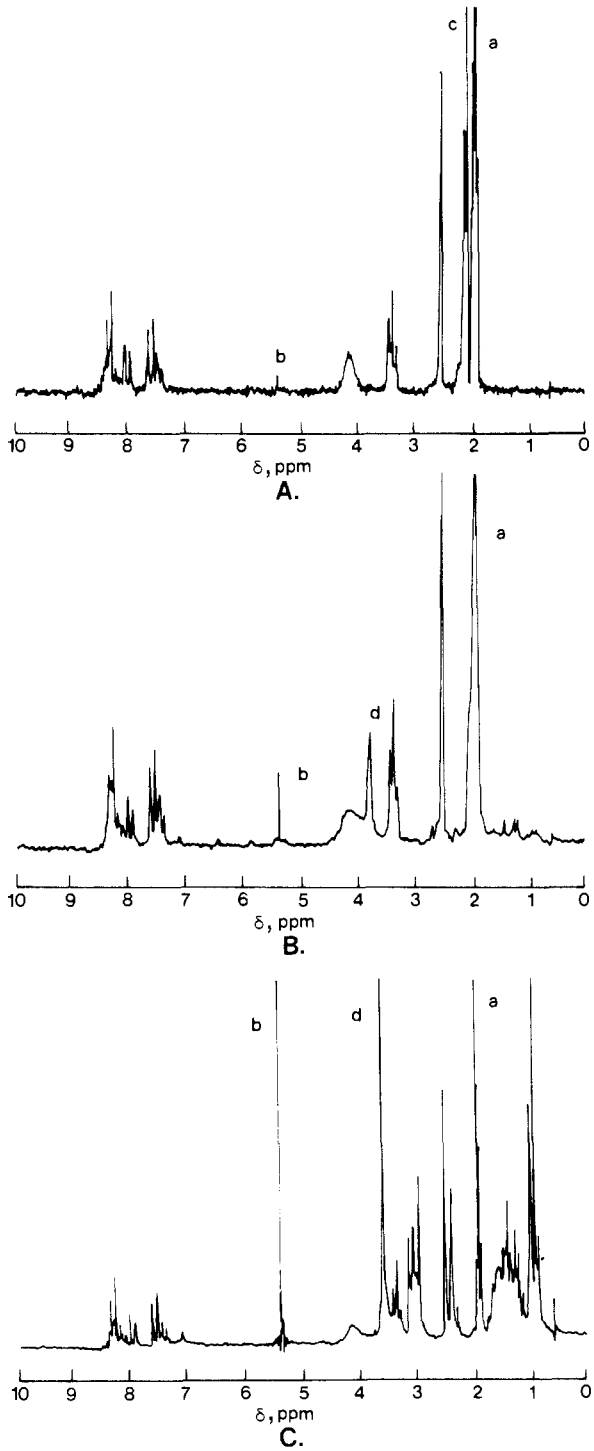

Figure 4. ^1H NMR spectra (90 MHz) of theoretical and actual product solutions of the ligand-substitution reaction of $[Cu^I((py)_2DAP)]^+$ with Zn^{2+} in CD_3CN: (A) authentic $[Zn^{II}((py)_2DAP)]^{2+}$; (B) $[Cu^I((py)_2DAP)]^+ + [Zn^{II}(CH_3CN)_6]^{2+}$; (C) $[Cu^I((py)_2DAP)]^+ + [Zn^{II}(H_2O)_6]^{2+}$. Extraneous peaks are labeled as follows: (a) protonated solvent in the CD_3CN; (b) contaminant CH_2Cl_2 from the drybox atmosphere; (c) water; (d) $[Zn^{II}(CH_3CN)_6]^{2+}$. Shifts were referenced by assignment of the solvent peak (a) at $\delta = 1.95$ vs internal TMS.

changes observed in the stopped-flow studies for both $[Cu^I((py)_2DAP)]^+$ and $[Cu^I((imidH)_2DAP)]^+$ were also consistent with ligand transfer to Zn(II). Thus, reaction 2 describes the ligand substitution reactions in this study, where L = (py) and (imidH):

$$[Cu^I(L_2DAP)]^+ + Zn^{2+} \rightarrow [Zn^{II}(L_2DAP)]^{2+} + Cu^+ \quad (2)$$

(B) Metal-Exchange Rate Measurements. The reaction of $[Cu^I((py)_2DAP)](BF_4)$ with excess $[Zn^{II}(CH_3CN)_6](BF_4)_2$ in CH_3CN at 20 mM ionic strength occurred with pseudo-first-order

Table I. Concentration Dependence of Observed Rate of Ligand Substitution at Constant Ionic Strength[a] in CH_3CN at 25 °C[b] for the Reaction $[Cu^I((py)_2DAP)]^+$ + Excess Zn(II), with Theoretical $\Delta A = 0.14$

$[Zn^{2+}]$, mM	k_{obs}, s^{-1}	% ΔA	$[Zn^{2+}]$, mM	k_{obs}, s^{-1}	% ΔA
A. μ = 20 mM, $[Zn(CH_3CN)_6]^{2+}$					
0.25[d]	98 ± 3	54	1.0	200 ± 10	43
0.50	153 ± 5	50	1.5	232 ± 9	43
B. μ = 10 mM,[c] $[Zn^{II}(H_2O)_6]^{2+}$					
0.25[d]	49 ± 3	86	1.5	119 ± 7	64
0.50	74 ± 4	78	2.0	132 ± 7	57
1.0	105 ± 5	64	2.5	140 ± 10	51

[a] Effective ionic strength, μ_e, was determined by allowing for the ion pairing of n-Bu_4NBF_4 in CH_3CN; K_{IP} = 10 M^{-1}.[15] [b] Initial concentration of copper(I) held at 0.05 mM unless noted otherwise. 10-mm path length. [c] Uncorrected for ion-pairing effects. When these effects are considered, by using K_{IP} = 10 M^{-1} for n-Bu_4NBF_4 and estimates of $K_{IP} \geq 126$ M^{-1} for $[Zn^{II}(H_2O)_6](BF_4)_2$,[16] these values of μ_e will show larger deviations than those at μ = 20 mM. It is known[16] that the ion pairing increases with increasing water content, but no exact function is available, nor is the water concentration of these experiments. [d] Initial copper(I) concentration lowered to 0.025 mM to keep zinc concentration in 10-fold excess.

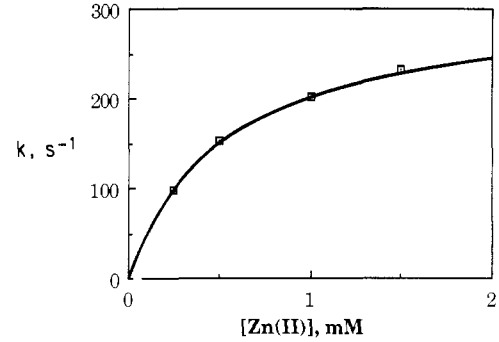

Figure 5. Dependence of the rate of ligand substitution upon the concentration of excess $[Zn^{II}(CH_3CN)_6]^{2+}$ in its reaction with $[Cu^I((py)_2DAP)]^+$ in CH_3CN at 25 °C. Solid line is the fit according to eq 3.

kinetics. The data are listed in Table I and are plotted in Figure 5. Also listed in Table I is the observed change in absorbance at 480 nm during each reaction, expressed as the % ΔA of the theoretical value, $\Delta A = 0.14$, determined from the extinction coefficient of $[Cu^I((py)_2DAP)]^+$ ($\epsilon_{480\ nm}$ = 2800 M^{-1} cm^{-1}), the fixed concentration of 0.05 mM, and the observation path length of 1 cm. These ΔA values are considerably smaller than the theoretical values but are accounted for by a substantial fraction of the reaction occurring during the estimated dead time, t_d, of the stopped-flow apparatus.[20]

As the $t_{1/2}$ values approach the value of the estimated t_d, the measured k_{obs} values possibly become less reliable, since the observed decay depends more upon the latter part of the reaction ($t_0 \approx$ second or third half-life at best). Therefore, the curvature of the plots of k_{obs} vs $[Zn^{2+}]$ could possibly be an artifact of this dead time effect. However, the semilog fits of log $(A_t - A_\infty)$ appear to be rigorously linear, indicating a lack of interfering reactions in the latter half-lives and thus that reliable values were obtained in these measurements. The saturation behavior seen in Figure 5 is reflected in the good linearity of a plot of $1/k_{obs}$ vs $1/[Zn^{2+}]$. Another artifact that can lead to apparent saturation kinetics at very high rates has recently been discussed by Dickson and Margerum.[21] This effect arises from the efficiency of mixing

(20) An estimate of t_d was obtained from the data in Table IB, which shows a larger range of ΔA values than the other reactions in the series. At the lowest rate, with $t_{1/2}$ = 14 ms, a ΔA value of 86% was observed. If it is assumed that the ΔA value of 51%, obtained for the fastest reaction in the series, is due to the instrumental dead time alone, then $t_d = t_{1/2}$ = 4.9 ms. This value of t_d would easily account for the small % ΔA values seen in Table I.

(21) Dickson, P. N.; Margerum, D. W. *Anal. Chem.* **1986**, *58*, 3153–3158.

Table II. Variation of $1/T_2$ with the Concentration of Cu(II) in the $[Cu^{I/II}((imidH)_2DAP)]^{+/2+}$ System[a]

$[Cu^{II}]$, mM	$1/T_2$,[b] Hz	$[Cu^{II}]$, mM	$1/T_2$,[b] Hz
0.0	12.2	0.6	19.9
0.2	13.2	0.8	22.3
0.4	15.7		

[a] In CD_3CN with [Cu(I)] = 7.32 mM, μ = 22.3 mM (Me_4NBF_4) at 25 °C. [b] By the line width $\Delta\nu_{1/2}$ of the imidazole C-5 proton resonance. Least-squares slope = (1.31 ± 0.16) × 10^4 M^{-1} s^{-1}, intercept = 11.3 ± 0.1 Hz.

of the stopped-flow instrument. Calibration of our instrument for aqueous reactions has shown that the mixing rate is fast enough that the saturation behavior that we observe is affected only to a minor degree by the mixing rate.

The above results are consistent with the rate law

$$\frac{-d[Cu^{I}((py)_2DAP)]}{dt} = \frac{ab[Cu^{I}((py)_2DAP)][Zn^{II}(CH_3CN)_6]}{1 + b[Zn^{II}(CH_3CN)_6]} \quad (3)$$

The intercept, $1/a$, of the double reciprocal plot yields a = 310 s^{-1} and the slope, $1/ab$, yields $b = 1.85 \times 10^3$ M^{-1}. Correction of these results for the mixing rate effect discussed above would lead to a slightly enhanced value for a.

When this reaction was carried out with $[Zn(H_2O)_6]^{2+}$ similar kinetics results were obtained, as shown in Table I. Although saturation behavior is again seen, the slope and intercept are somewhat different from those for the reaction with $[Zn(CH_3CN)_6]^{2+}$. Since hydrolysis or some other decomposition occurs in this reaction, these studies were not pursued further.

The reaction of $[Zn^{II}(CH_3CN)_6]^{2+}$ with $[Cu^{I}(imidH)_2DAP)]^{+}$ was too fast to observe in CH_3CN with the Cu(I) concentration at 0.05 mM, the Zn(II) concentration at 1.0 mM, and μ = 10 mM. If it is assumed that the reaction has a rate law of the same form as for the reaction with $[Cu^{II}((py)_2DAP)]^{+}$, then the rapid rate may be due to greater values for a, b, or both.

Electron-Self-Exchange Rate of $[Cu((imidH)_2DAP)]^{n+}$. In a fashion similar to the previous measurement[7] of the electron-self-exchange rate of $[Cu^{I/II}((py)_2DAP)]^{n+}$, k'_{11}, the electron-self-exchange rate, k'_{22}, for the $[Cu^{I/II}((imidH)_2DAP)]^{n+}$ couple was measured by using the line-width ($\Delta\nu_{1/2}$) method for the determination of $1/T_2$. The subscript designations from the previous work are retained here for consistent terminology. The exchange rate is related to $1/T_2$ according to

$$\pi\Delta\nu_{1/2} = 1/T_2 = 1/T_{2n} + 1/T_{2e} = k'_{22}[Cu^{II}((imidH)_2DAP)^{2+}] + 1/T_{2n} \quad (4)$$

which is valid in the slow-exchange regime.[18] In this equation, $1/T_{2n}$ represents the natural transverse relaxation time and $1/T_{2e}$ represents the exchange contribution to the relaxation time. The $\Delta\nu_{1/2}$ (fwhm) of the resonance of the imidazole proton in the 5-position (see Figure 1) was measured. Decoupling of a weak homonuclear interaction was necessary to reduce this resonance to a singlet and was achieved by irradiating the broad imidazole N proton resonance at δ = 10–11. Data for the $1/T_2$ measurements made at varied Cu(II) concentration are presented in Table II. The chemical shift was independent of [Cu(II)], as expected. The experimental value for k'_{22} as determined from a plot of $1/T_2$ vs [Cu(II)] is (1.31 ± 0.16) × 10^4 M^{-1} s^{-1} at μ = 22.3 mM and 25 °C with $1/T_{2n}$ = 11.3 ± 0.1 Hz. The larger value obtained for $1/T_{2n}$ in this experiment compared with the results presented in our previous paper[7] is attributable to the higher field inhomogeneity of the JEOL FX-90Q instrument when compared to the IBM 300-MHz instrument.

Discussion

The X-ray crystal structure of $[Cu^{II}((imidH)_2DAP)]^{2+}$ shows that the complex is pentacoordinate, with all five Cu–N bonds of comparable length. This general structure is also inferred from the EXAFS data for the solution state. In the case of the Cu(I) complex, the crystal structure shows that the two arms of the ligand are inequivalent, with the two Cu–N imino bonds being substantially weaker than the others and one of the two being much longer than the other. The presence of two Cu–N bonds much longer than the others is likewise consistent with the EXAFS data. The NMR spectrum of the Cu(I) complex shows that the two arms of the ligand are equivalent at room temperature, so there must be a rapid dynamic process that leads to the equivalence.

Substitution Reactions. In view of the above dynamic behavior, studies of the substitution reactions of the two Cu(I) complexes were undertaken. It was found that reactions with the phenanthrolines occur in a two-step process, with the first step being too fast to monitor. Since the complexes are pentacoordinate, it is quite possible that these reactions occur by an associative mechanism, and thus they do not reveal anything regarding the mechanism of the spontaneous dynamic process.

Studies of the reactions of the Cu(I) complexes with solvated metal ions were undertaken under the assumption that an associative mechanism could not occur. Of these, the reaction of $[Cu^{I}((py)_2DAP)]^{+}$ with $[Zn(CH_3CN)_6]^{2+}$ in CH_3CN yielded meaningful kinetics results. The saturation rate law shown in eq 3 is consistent with two conceivable mechanisms, shown in eq 5–8.

mechanism 1

$$CuL_2^{+} \rightleftarrows LCuL^{+} \quad k_d, k_{-d}, K_d \quad (5)$$

$$LCuL^{+} + Zn^{2+} \rightarrow Cu^{+} + ZnL_2^{2+} \quad k_x \quad (6)$$

Here K_d refers to the partial dissociation of the Cu(I) complex to form an intermediate in low enough concentration to be spectroscopically undetectable. Either ligand dissociation or zinc binding can be rate-limiting, depending on the conditions.

mechanism 2

$$CuL_2^{+} + Zn^{2+} \rightleftarrows LCuLZn^{3+} \quad K_m \quad (7)$$

$$LCuLZn^{3+} \rightarrow Cu^{+} + ZnL_2^{2+} \quad k_z \quad (8)$$

This mechanism implies that there is a different intermediate, $LCuLZn^{3+}$, formed in a rapid preequilibrium by the bridging of Cu and Zn by the ligand, and that breakdown of this intermediate is the rate-limiting step.

The rate law for the first mechanism is obtained by using the steady-state approximation

$$-d[CuL_2]/dt = k_d k_x[Zn^{2+}][CuL_2]/(k_{-d} + k_x[Zn^{2+}]) \quad (9)$$

which implies a form consistent with the observed saturation behavior

$$1/k_{obs} = k_{-d}/k_d k_x[Zn^{2+}] + 1/k_d \quad (10)$$

The second mechanism leads to simple behavior when the two species CuL_2 and $LCuLZn^{3+}$ are spectroscopically indistinguishable; i.e.

$$k_{obs} = k_z K_m[Zn^{2+}]/(1 + K_m[Zn^{2+}]) \quad (11)$$

This form is also consistent with the observed saturation behavior

$$1/k_{obs} = 1/(k_z K_m[Zn^{2+}]) + 1/k_z \quad (12)$$

Under the conditions of high $[Zn^{2+}]$ this mechanism requires that the equilibrium with K_m be shifted largely to the right. In order for the ligand in $[Cu^{I}(py)_2DAP]^{+}$ to bridge to Zn^{2+}, the terminal pyridinyl moiety must dissociate from the Cu(I) and bind to the Zn(II). Such a process would be expected to lead to a substantial change in the electronic spectrum. The fact that no such change was observed is taken in support of mechanism 1. Thus the rate-limiting process at high concentrations of Zn^{2+} is inferred to be disengagement of one arm of the ligand from Cu(I). This allows us to identify the experimental parameter a as k_d, and thus k_d has the value 310 s^{-1}.

In the case of the reaction of $[Cu^{I}((imidH)_2DAP)]^{+}$ with $[Zn(CH_3CN)_6]^{2+}$, which was too rapid to monitor, it is quite possible that the rate law is of the same form as for the reaction of $[Cu((py)_2DAP)]^{2+}$. A decreased value for k_{-d} or increased

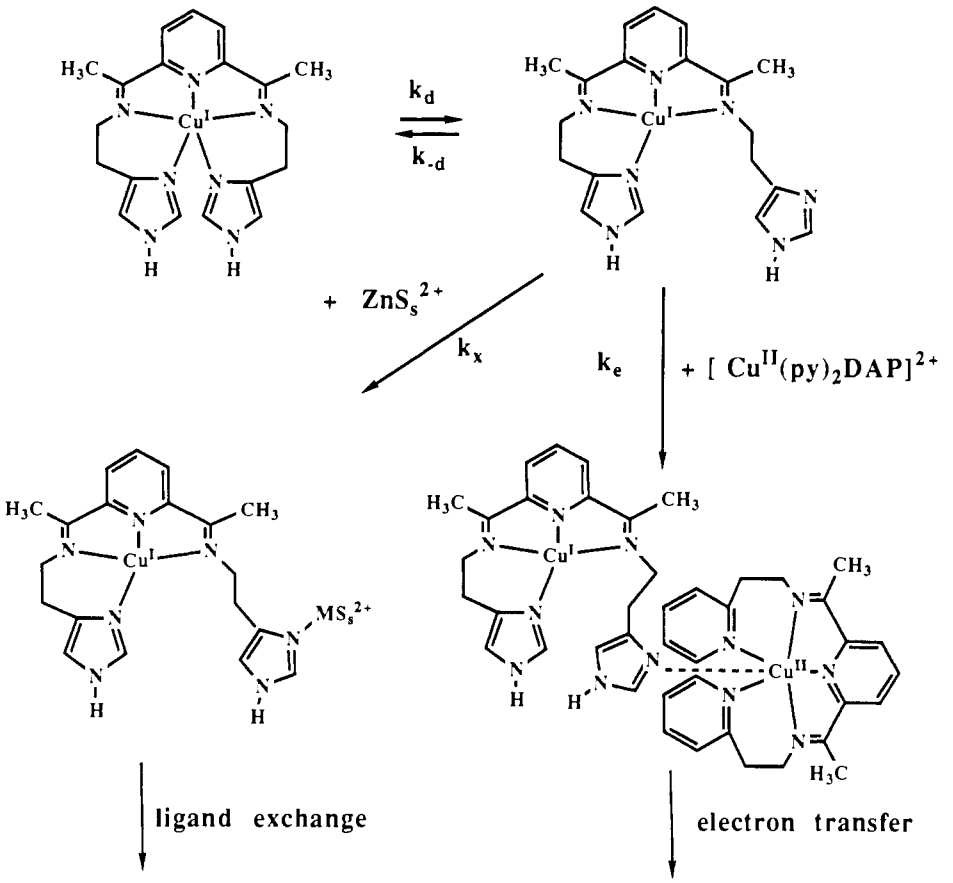

Figure 6. Schematic representation of the metal-substitution reaction by mechanism 1, ZnS_s^{2+} + $[Cu^I((imidH)_2DAP)]^+$, and of the hypothetical inner-sphere mechanism of electron transfer.

values for k_x and k_d could lead to the reaction occurring in the dead time of the stopped-flow; in other words, a value of 310 s^{-1} for k_d is not incompatible with the observed behavior in this system as well. Furthermore, that this rate constant is similar in magnitude to the rate constant for the racemization observed in the temperature-dependent NMR study of $[Cu^I((py)_2DAP)]^+$ in CD_2Cl_2 at −20 °C supports the notion that the mechanism leading to racemization is also disengagement of one ligand arm.

This study appears to be the first on the substitution kinetics of pentacoordinate Cu(I). In fact, there are only a few substitution kinetic studies of Cu(I) in any environment. Notable among these is a pulse-radiolytic investigation of the reaction of aqueous Cu^+ with fumarate and maleate, in which the rate constant for dissociation of these ligands was measured at $\approx 2 \times 10^5$ s^{-1}.[22] In another aqueous study the rate constant for dissociation of 1,10-phenanthroline from $[Cu(phen)_2]^+$ was determined to be 0.2 s^{-1}.[23] The only data reported in nonaqueous solution are in a 90:10 mixture of acetonitrile and water; the complexes are a series of Cu(I) bis chelates of phenanthrolines, especially those in which the ligands are intertwined rings that form "catenates".[24] In these systems the rate constants for spontaneous decomplexation range from a high of 4.8 s^{-1} for the 2,9-dimethylphenanthroline system to values too slow to measure in some of the catenates. Our work appears to be the first report of the kinetics of displacement of Cu(I) by another metal ion.

Electron-Transfer Reactions. In this study and in our previous investigation of electron-transfer kinetics in pentacoordinate Cu(I)/Cu(II) systems, we have used NMR line-broadening measurements to determine self-exchange rates. The rate constants have been determined under the assumption that the "slow-exchange" limit applies. Groeneveld et al. have recently shown that this can be a risky assumption.[25] These workers found that a discrepancy in the literature of 2 orders of magnitude in the self-exchange rate constant for azurin could be traced to the fact that one of the research groups examined a proton resonance that was in the fast-exchange regime although they assumed it to be in the slow-exchange regime. This error led to a calculated rate constant that is slower than the actual rate constant. Methods to test which regime is dominant for a given system include considerations of T_1 of the Cu(II) complex and the dependence of T_2 of the Cu(I) complex on [Cu(I)] and temperature. We were not able to detect an NMR spectrum of the Cu(II) complex, so the first method is not applicable, and in future studies we plan to test all our copper systems with regard to the second approach. In the meantime, an attempt to resolve the issue is presented below in the discussion of Marcus theory.

Inner-Sphere Electron Transfer? Certainly an outer-sphere mechanism is an attractive possibility for the electron-transfer reaction, but an inner-sphere mechanism must also be considered. The most likely pathway for an inner-sphere process is illustrated in Figure 6. This figure highlights the similarity of this mechanism to that discussed above for the metal-substitution reaction. Thus, an arm of the ligand on Cu(I) detaches and binds to the copper center of a Cu(II) complex, and electron transfer ensues in the binuclear intermediate. In such a mechanism the maximum rate at high [Cu(II)] will be the rate of detachment from Cu(I), which has a rate constant of 310 s^{-1} for $[Cu^I((py)_2DAP)]^+$. In the NMR line-broadening experiments reported previously,[7] the highest attained value of $k'_{11}[Cu^{II}((py)_2DAP)^{2+}]$, the pseudo-first-order rate constant, was 9 s^{-1}, and so the substitution kinetics does not rule out an inner-sphere mechanism for electron transfer.

(22) Meyerstein, D. *Inorg. Chem.* **1975**, *14*, 1716–1717.
(23) Hodges, H. L.; de Araujo, M. A. *Inorg. Chem.* **1982**, *21*, 3236–3239.
(24) (a) Albrecht-Gary, A.-M.; Saad, Z.; Dietrich-Buchecker, C. O.; Sauvage, J.-P. *J. Am. Chem. Soc.* **1985**, *107*, 3205–3209. (b) Albrecht-Gary, A.-M.; Dietrich-Buchecker, C.; Saad, Z.; Sauvage, J.-P.; Weiss, J. *J. Chem. Soc., Chem. Commun.* **1986**, 1325–1327. (c) Dietrich-Buchecker, C. O.; Edel, A.; Kintzinger, J. P.; Sauvage, J. P. *Tetrahedron* **1987**, *42*, 333–344.
(25) Groeneveld, C. M.; Dahlin, S.; Reinhammar, B.; Canters, G. W. *Recl.: J. R. Neth. Chem. Soc.* **1987**, *106*, 279.

A similar conclusion can be reached for the present $[Cu((imidH)_2DAP)]^{2+/+}$ system.

As envisioned above, the inner-sphere mechanism has an asymmetric transition state. In other words, before electron transfer the binuclear intermediate has four-coordinate Cu(I) and six-coordinate Cu(II), whereas after electron transfer, Cu(II) will be four-coordinate and Cu(I) will be six-coordinate. The reaction is degenerate, and so if the transition state is asymmetric, there must be two mirror-image pathways proceeding at equal rates. Thus, there must be a pathway in which an arm of the ligand detaches from Cu(II) and binds to Cu(I), and this substitution process must be sufficiently facile to occur as a rapid preequilibrium prior to electron transfer. Unfortunately, we do not have any data pertaining to the rates of substitution in our Cu(II) complexes. Given the generally observed preference of Cu(I) for lower coordination numbers and the general pattern that substitution rates decrease with increasing oxidation state, it is reasonable to assume that the rate of ligand dissociation in our Cu(II) complexes is several orders of magnitude less than in the corresponding Cu(I) complexes. If this is the case, then the inner-sphere mechanism can be ruled out; such experiments are planned in a future study.

Irrespective of substitution rates it is difficult to perceive a kinetic advantage for the inner-space mechanism relative to the outer-sphere mechanism, because the former would provide a bridge containing a saturated ethylene linkage. For this reason as well as the considerations expressed above concerning substitution rates, we presently favor an outer-sphere mechanism.

Outer-Sphere Electron Transfer? We have reported[7] stopped-flow results for the cross exchange of $[Cu^{II}((py)_2DAP)]^{2+}$ with $[Cu^{I}((imidH)_2DAP)]^{+}$ and NMR T_2 studies of the self-exchange reaction for the $[Cu((py)_2DAP)]^{2+/+}$ couple. An estimate of the self-exchange rate constant for the $[Cu((imidH)_2DAP)]^{2+/+}$ couple was performed by applying the cross relationship of the Marcus theory under the assumptions that the reaction mechanisms were all outer sphere and that the NMR data were obtained in the slow-exchange regime. The present NMR investigation of the $[Cu((imidH)_2DAP)]^{2+/+}$ system permits a test of these assumptions.

In our previous stopped-flow study, medium effects were investigated in detail. It was found that ion pairing occurred to a significant degree under the conditions of the present experiments. The data were treated by a rate law in which ion pairing of the background electrolyte and the Cu(II) complex was taken into account in calculating the ionic strength and in which the ion-paired Cu(II) complex was unreactive. The effects of ion pairing largely cancel in calculations with the Marcus cross relationship, but for the sake of rigor we prefer the results in which these effects are taken into account.

An essential component of the calculations is the equilibrium constant for the cross reaction. This is available from our prior study, corrected for ion-pairing effects, at μ = 38 mM. Thus the rate constants are corrected to the same conditions as follows. A value for k°_{22} (μ = 0) is calculated from our experimental value for k'_{22} by using the expression

$$k'_{22} = \frac{k^{\circ}_{22}(\exp(4A\mu^{1/2}/(1 + Ba\mu^{1/2})))}{1 + K_{IP2}[BF_4^-](\exp(-4A\mu^{1/2}/(1 + Ba\mu^{1/2})))} \quad (13)$$

in which A = 1.646 $M^{-1/2}$, $B = (8\pi Ne^2/1000\epsilon k_B T)^{1/2}$ = 0.486 $M^{-1/2}$ Å^{-1},[26] and a is the ion size parameter maintained at 3.5 Å.[27]

(26) Robinson, R. A.; Stokes, R. H. *Electrolyte Solutions*, 2nd ed.; Academic: New York, 1959; p 230.

(27) Estimated from the values for several $[n\text{-}Bu_4N]^+$ salts in CH_3CN given in: Fernandez-Prini, R. In *Physical Chemistry of Organic Solvent Systems*; Covington, A. K., Dickenson, T., Eds.; Plenum: London, 1973. The values for $[n\text{-}Bu_4N]Br$ (3.5 Å), $[n\text{-}Bu_4N]ClO_4$ (3.57 Å), $[n\text{-}Bu_4N]NO_3$ (3.73 Å), and $[n\text{-}Bu_4N]I$ (3.6 Å) were relatively independent of the anion, while the values for $[n\text{-}Bu_4N]Pic$ (4.0 Å) and $[n\text{-}Bu_4N]B(C_6H_5)_4$ (4.5 Å) show a large deviation from these, due to their bulk. Clearly, the relatively small BF_4^- salt would fall into the first category. Variations in size of $[R_4N]^+$ cation led to slightly greater variations in the ion size parameter. The reported value of a for $NaBPh_4$ is 5.2 Å.

Table III. Changes of Bond Length Associated with the Oxidation States of $[Cu((py)_2DAP)]^{n+}$ [7] and $[Cu((imidH)_2DAP)]^{n+}$ [9,10]

	Δd(Cu(II) → Cu(I)), Å	
	$[Cu((py)_2DAP)]^{n+}$	$[Cu((imidH)_2DAP)]^{n+}$
central pyridine	+0.174 (34)	−0.023 (83)
terminal rings	−0.001 (32)	−0.102 (79)
	−0.046 (32)	−0.151 (91)
imino	+0.214 (32)	+0.464 (79)
	+0.263 (33)	+0.224 (81)

The dielectric constant, ϵ, is 35.95,[26] k_B is the Boltzman constant, and K_{IP2}, determined previously, is 100 M^{-1}. k''_{22} (at μ = 38 mM, corrected for ion pairing) is then given by

$$\log k''_{22} = \log k^{\circ}_{22} + 4A\mu^{1/2}/(1 + Ba\mu^{1/2}) \quad (14)$$

which leads to a value for k''_{22} of 2.8 × 10^4 M^{-1} s^{-1}. Similar calculations reported previously gave a value for k''_{11} of 2.8 × 10^3 M^{-1} s^{-1}. The equilibrium constant, K''_{12}, also reported previously, has a value of 283.

With these data in hand we can now use the cross relationship of the Marcus theory to calculate a theoretical value for k''_{12}. The equations used are

$$k_{12} = (k_{11}k_{22}K_{12}f_{12})^{1/2} \quad (15)$$

$$\ln f_{12} = (\ln K_{12})^2/(4 \ln (k_{11}k_{22}/Z^2)) \quad (16)$$

where a value of 10^{11} M^{-1} s^{-1} is used for Z. The outcome is a value of 1.3 × 10^5 M^{-1} s^{-1} for $k''_{12,calc}$, which may be compared with the experimental value of 9.8 × 10^4 M^{-1} s^{-1}.

That the agreement between $k''_{12,calc}$ and k''_{12} is excellent is at present our best evidence that the NMR data were collected in the slow-exchange regime. The agreement may also be taken in support of the argument that the mechanism of electron transfer is outer-sphere, although here the evidence is not as clear, since certain inner-sphere reactions have been shown to obey the Marcus cross relationship.[28] In conclusion, the evidence is not definitive that the reactions are outer sphere, but the weight of the Marcus calculations, the substitution kinetics, and the saturated ethylenic linkage in the ligand lead to the reasonable belief that this is the case.

It is of some interest to consider the magnitudes of the self-exchange rate constants. The values are summarized here: k''_{11} = 2.8 × 10^3 M^{-1} s^{-1}, k''_{22} = 2.8 × 10^4 M^{-1} s^{-1}, and k''_{33} = 3.1 × 10^4 M^{-1} s^{-1}. These values do not differ much from those reported previously. As we noted then, the 10-fold greater value for k''_{33} than for k''_{11} can be rationalized on the basis that the greater bulk of $[Cu((imidR)_2DAP)]^{n+}$ leads to a reduced solvent reorganizational energy. The fact that k''_{22} is a factor of 10 greater than k''_{11} is more difficult to rationalize. In our previous paper it was suggested that the effect may have been due to the combined effects of experimental error and the approximations inherent in the Marcus cross relationship; the present data show that the effect is real. If the effect is to be attributed to a reduced internal reorganizational energy, then a complete treatment would entail knowing the structures and force fields of the complexes. The force fields are unknown at this time, but perhaps some hints about the reorganizational energies can be obtained by considering the crystallographically determined structural changes.

Bond length changes as a function of oxidation state for the $[Cu((py)_2DAP)]^{n+}$ and $[Cu((imidH)_2DAP)]^{n+}$ redox couples are presented in Table III, in which it can be seen that the two systems are quite different. In the $[Cu((py)_2DAP)]^{2+/+}$ system the central pyridine and the two imino nitrogens move as a unit with the change in oxidation state. On the other hand, in the $[Cu((imidH)_2DAP)]^{2+/+}$ system the motion is more complex, including features that might be described as conformational in character. It is conceivable that a different conformation of only slightly

(28) Gould, E. S. *Inorg. Chem.* **1979**, *18*, 900–901.

increased energy may exist for one of the oxidation states so that the structural difference between it and the other oxidation state is relatively small. The mechanism of the electron-transfer reaction would then be successive conformational change and electron transfer. A mechanism quite similar to this has recently been proposed for the electron-transfer reactions of a series of copper-polythia ether complexes.[29]

A more general lack of correlation between structural changes and self-exchange rate constants in Cu(I)/Cu(II) systems is evident when the behavior of the $[Cu(TAAB)]^{+/2+}$ couple is considered. This couple has a very large self-exchange rate constant of 5×10^5 M^{-1} s^{-1} despite its change in coordination number between the two oxidation states.[30] Perhaps a sequential mechanism is at work here also. This concept could have important consequences in cuproprotein chemistry, in that it would not be necessary for the protein to impose a rigid coordination environment in order to attain facile electron transfer.

Several reports of electron-transfer reactions involving synthetic Cu(I)/Cu(II) couples have appeared since our last publication. These include studies of the polythia ether systems in aqueous solution mentioned above.[29] There are two reports on redox reactions of copper complexes with ruthenium ammine and bipyridyl complexes in aqueous solution and in 50% methanol.[31,32] There is also a report of the reactions of several tetracoordinate copper(II) complexes with ferrocene and 1,1'-dimethylferrocene in acetonitrile.[33] The ferrocene reactions displayed saturation kinetics at high $[Fe(cp)_2]$, which was interpreted in terms of a mechanism involving extensive association of the two reactants. In the studies with the ruthenium complexes, it was deduced that the coordination number about copper changed from 4 to 5 with increasing oxidation state. The polythia ether ligand systems showed quite different self-exchange rate constants, depending on whether the complexes were being reduced or oxidized; a "square" scheme was devised to account for this behavior. Thus, none of these recent studies are directly comparable with the reactions described in the present work.

Much more pertinent is the recent study by Groeneveld et al. of $Cu(bidhp)^{n+}$.[18b] In the Cu(I) state this is a pseudotetrahedral complex bearing a linear tetradentate N_2S_2 ligand. The Cu(II) analogue apparently also bears a bound aquo ligand in the solid state, but it is claimed that in DMSO solution both the Cu(I) and Cu(II) states are bound solely by the N_2S_2 ligand. Dynamic NMR techniques were used to extract a self-exchange rate constant of 4×10^3 M^{-1} s^{-1} in DMSO at 28 °C. Unfortunately it is difficult to assess the degree of structural reorganization in this system because the crystal structure of the tetracoordinate Cu(II) derivative is not yet available.

Conclusions. The present studies confirm the previous estimate of the electron self-exchange rate constant for the $[Cu((imidH)_2DAP)]^{2+/+}$ redox couple and demonstrate excellent agreement with Marcus theory. Unfortunately, there is still some uncertainty as to whether the mechanism is outer-sphere. Perhaps this issue can be resolved by measuring the substitution kinetics of the Cu(II) complexes. Other methods may actually be more direct, such as using (1) rigorously outer-sphere reaction partners with known self-exchange rates to verify the self-exchange rates for the copper complexes by the Marcus treatment or (2) derivatives of the $[Cu(L_2DAP)]^{n+}$ molecules with macrocyclic ligands designed to prevent the ligand dissociation step entirely. These efforts are in progress, with the objective of obtaining a firmer understanding of the interrelationships between structure, conformational mobility, and reaction rates of these and related model compounds.

Acknowledgment. This research was supported by the NSF (D.M.S., Grant CHE-8520515), the NIH (L.J.W., Grant GM-28451), and the Robert A. Welch Foundation (D.M.S., Grant C-846, and L.J.W., Grant C-627). We are grateful to Dr. A. Kook for help with the NMR spectra, to DeAnna Coggin for assistance during manuscript preparation, and to Prof. Geoffrey Davies for helpful conversations. The XAS work reported herein was performed at the Stanford Synchrotron Radiation Laboratory, which is supported by the Department of Energy, Office of Basic Energy Sciences, and the National Institute of Health, Biotechnology Resource Program, Division of Research Resources. R.A.S. is a NSF Presidential Young Investigator and an Alfred P. Sloan Research Fellow.

Registry No. $[Cu^I((imidH)_2DAP]^+$, 69021-97-2; $[Cu^I((py)_2DAP)]^+$, 75688-55-0; $[Zn^{II}(CH_3CN)_6]^{2+}$, 21519-23-3.

(29) Martin, M. J.; Endicott, J. F.; Ochrymowycz, L. A.; Rorabacher, D. B. *Inorg. Chem.* **1987**, *26*, 3012-3022.
(30) Pulliam, E. J.; McMillin, D. R. *Inorg. Chem.* **1984**, *23*, 1172-1175.
(31) Davies, K. M.; Guilani, B. *Inorg. Chim. Acta* **1987**, *127*, 223-227.
(32) Davies, K. M.; Byers, B. *Inorg. Chem.* **1987**, *26*, 2823-2825.
(33) Aoi, N.; Matsubayashi, G.-E.; Tanaka, T. *Polyhedron* **1987**, *6*, 943-946.

Contribution from the Departments of Chemistry Education and Chemistry, Seoul National University, Seoul 151-742, Korea

Effects of Transition-Metal Ions on the Reduction of Di-2-pyridyl Ketone with Sodium Borohydride

Myunghyun Paik Suh,*[1a] Chee-Hun Kwak,[1b] and Junghun Suh*[1b]

Received February 3, 1988

The Co(II) complexes of di-2-pyridyl ketone (dpk), di-2-pyridylcarbinol (dpc), and di-2-pyridylmethanediol (dpk-H_2O) were prepared and characterized. In methanol, the Co(II) complex of dpk $[Co(dpk)_3](ClO_4)_2 \cdot 3H_2O$ was reduced with $NaBH_4$, yielding $[Co(dpc)_3](ClO_4)_2$, and was hydrated to give $[Co(dpk\text{-}H_2O)_3](ClO_4)_2 \cdot {}^3/_2CH_3OH$. Kinetics of the reduction of dpk with $NaBH_4$, yielding dpc, were studied in ethanol containing 14% (v/v) diglyme in the presence of Co(II) or Zn(II) ion and in the absence of the divalent metal ions. The catalytic effects of the Zn(II) ion are attributed to the inductive effects of the metal ion acting as a Lewis acid, leading to enhancement in the electrophilicity of the carbonyl group of the coordinated dpk. On the other hand, the Co(II)-promoted reduction of dpk with $NaBH_4$ involves two successive intermediates containing Co(I) ion. From the rate data observed for the conversion of the first intermediate into the second one, the structures of the two intermediates were assigned. Thus, the Co(II)-promoted reduction of dpk with $NaBH_4$ appears to involve the initial reduction of the central metal ion with $NaBH_4$ and subsequent electron transfer from the metal ion to the carbonyl group of the coordinated dpk.

Introduction

Previously, we reported that the reduction of the Co(II) complex of di-2-pyridylamine (dpa) $[Co(dpa)_2Cl_2]$ with $NaBH_4$ under an inert atmosphere followed by oxidative addition with CH_3I led to the organometallic Co(III) complex $[Co(dpa)_2(CH_3)_2]I$.[2] In this reaction it was proposed that the reduction of the Co(II) complex with $NaBH_4$ initially produced the Co(I) species as an intermediate.

(1) (a) Department of Chemistry Education. (b) Department of Chemistry.
(2) Suh, M. P.; Oh, Y.-H.; Kwak, C.-H. *Organometallics* **1987**, *6*, 411.

0020-1669/89/1328-0050$01.50/0